Residual Stress and Viscoelastic Deformation of Film Insert Molded Automotive Parts

Seong Yun Kim, Sung Ho Kim, Hwa Jin Oh, Seung Hwan Lee, Jae Ryoun Youn

Department of Materials Science and Engineering, Research Institute of Advanced Materials (RIAM), Seoul National University, Sillim-Dong, Gwanak-Gu, Seoul 151-742, Korea

Received 31 December 2009; accepted 27 February 2010
DOI 10.1002/app.32371
Published online 29 June 2010 in Wiley InterScience (www.interscience.wiley.com).

ABSTRACT: Complex automotive parts were produced by film insert molding and the ejected parts were annealed to investigate the viscoelastic deformation. Warpage of the part was predicted by numerical simulation of mold filling, packing, and cooling stages with non-isothermal three-dimensional flow analysis. The flow analysis results were transported to a finite element stress analysis program and the stress analysis was performed by using time-temperature superposition principle to investigate viscoelastic deformation. Predicted residual stresses, viscoelastic deformation, and warpage showed good agreement with experimental results. Thermal shrinkage of the inserted film and relaxation of the residual stress affected the viscoelastic deformation of the part significantly during annealing. J Appl Polym Sci 118: 2530–2540, 2010

Key words: annealing; injection molding; residual stress; viscoelastic behavior; warpage

INTRODUCTION

Polymeric materials have been used in automotive industry and the total amount has been increased significantly. Because they have low density and excellent mechanical properties, polymers are used as raw materials for automotive parts to improve the fuel economy without sacrificing safety. For last decades, lighter and tougher automotive interior parts have been produced by the automotive industry. Because emotional design concept requires automotive parts with fine details, some automotive interior products are manufactured by film insert molding (FIM).

FIM is a new injection molding method in which molten polymer is filled into the cavity after a film is attached to one side of the mold walls. The inserted film is preformed and attached to the cavity wall for decoration of the part instead of traditional screen printing or painting. Surface quality of the injection molded products can be improved by the decorated film. Moreover, adhesion between the film and the substrate may be enhanced because the injected hot molten resin can re-melt the film partially.[1–4] FIM is preferred to other surface decoration methods because it is a one-step process without extra post-processing that will increase the production cost. Therefore, FIM has been widely applied to various products and will be explored continuously for production of automotive interior parts, cellular phone cases, logo design of plastic products, etc.

There are some disadvantages of the film insert molded products because there is a possibility of washing off of printed ink, unexpected weld line, wrinkling of the inserted film, non-uniform shrinkage, and warpage of the part. In particular, serious problems such as non-uniform shrinkage and warpage have been reported because they occurred frequently when the FIM was used for a large part with complex geometry. In general, non-uniform shrinkage is generated by complex mold geometry and can cause significant deformation of the geometry.[5] Although there have been many studies on warpage and shrinkage of injection molded parts[6–8] and film insert molded parts with simple geometry,[9–12] investigations on warpage of the film insert molded products with complex geometry seldom have been reported. Therefore, it is necessary to understand why the film insert molded parts may experience large deformation or fracture when the product is used long time or exposed to high temperature.

Numerical analysis is effective in understanding the processing procedure and physical properties of the final product beforehand. In the previous study,[9–12] numerical flow analysis was performed for the FIM process by using a commercial finite element analysis code (Moldflow) with the capability of part insert. Time-dependent viscoelastic stress analysis was also performed by using a commercial stress analysis code (ABAQUS)

Correspondence to: J. R. Youn (jaeryoun@snu.ac.kr).
Contract grant sponsor: National Research Foundation of Korea (NRF) grant funded by the Korean government (MEST) through the Intelligent Textile System Research Center (ITRC) and by the Hyundai Motor Company; contract grant number: R11-2005-065.

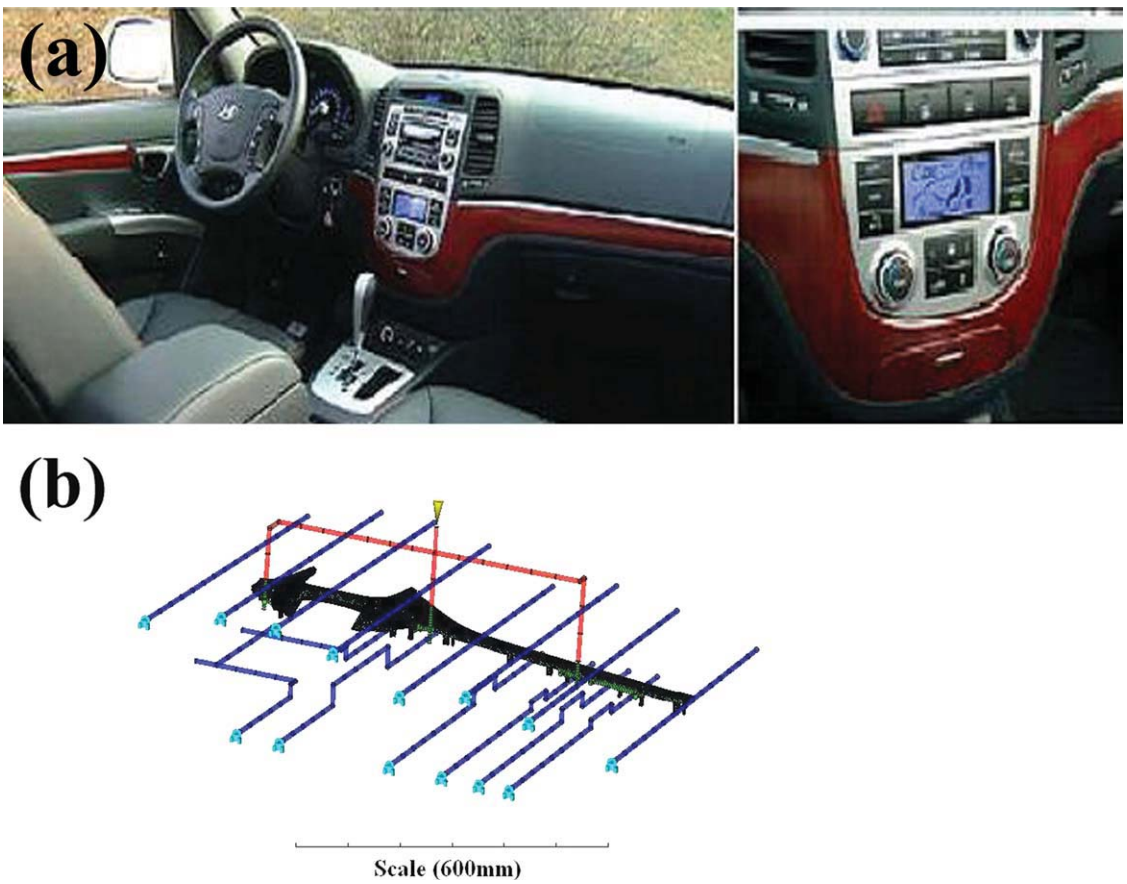

Figure 1 (a) Installed automotive interior part (center panel of Santa Fe model, Hyundai Motor Co., Korea). (b) Diagram of runner, multiple gates, cooling channel, and molded shape of the film insert molded automotive interior part. [Color figure can be viewed in the online issue, which is available at www.interscience.wiley.com.]

for flat and simple geometries. However, the numerical analysis has been rarely applied to huge, bulk, and complex automotive interior parts produced by FIM. Because the product considered in this study has the length of about 90 cm and numerous ribs, at least 400,000 finite elements were needed for three-dimensional flow and stress analyses.

Automotive interior parts were prepared by FIM in this study to investigate warpage of the parts and were annealed to evaluate the thermoviscoelastic deformation. Three dimensional flow and structural analyses were performed to predict residual stresses in the product and to evaluate long-term viscoelastic deformation of the film insert molded part by using time-temperature superposition principle. Weld line locations, residual stresses, and deformed geometry were obtained by the numerical analysis and the numerical predictions were compared with experimental results.

EXPERIMENTAL

Materials

The film used for FIM has a laminated structure that consists of acrylonitrile-butadiene-styrene (ABS) substrate and polymethylmetacrylate (PMMA) film. Thickness of the PMMA layer was 0.05 mm and that of the ABS layer was 0.45 mm when supplied by the manufacturer (Nissha printing Co., Japan). It is expected that biaxial molecular orientation and residual stresses were developed in the film during manufacturing process. The received film was preformed to fit the mold cavity by using thermoforming at 150°C because of complicate shape of the automotive part. The polymeric resin used for injection molding was a blend (STAROY HP-1000X, Cheil industries, Korea) of polycarbonate (PC) and ABS and had the MFR of 27.0 g/10 min at 250°C under the load of 10 kg according to ASTM D 128.

Characterization of materials

Dimensions of the thermoformed film and the annealed film treated at 80°C were measured. Linear thermal expansion coefficient, α, of the film was determined by the following equation.

$$\alpha = \frac{\Delta l}{l_0 \Delta T} \tag{1}$$

where Δl is expanded length, l_0 is initial length, and ΔT is temperature difference. For modeling of

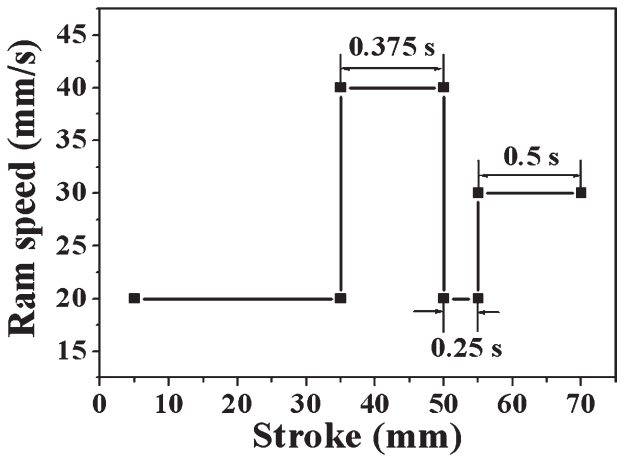

Figure 2 Injection speed used for FIM of the part with complex geometry as a function of ram stroke.

viscoelastic properties of materials, relaxation moduli of the film and substrate were measured by using the dynamic mechanical analysis (DMA 2980, TA instrument, New Castle, DE).

Film insert injection molding

The PC/ABS resin was dried at 80°C in a convection oven for 4 h before injection molding to minimize the effect of moisture. The film was attached to one side of the mold wall before injection of the resin. The polymer resin was injected into the cavity at 265°C by using an injection molding machine (Engel, Germany). Maximum clamped force and screw diameter of the machine were 120 ton and 28 mm, respectively. Maximum pressure and injection speed were 240 Mpa and 600 mm/s, respectively. The injection process was performed by using runners, multiple gates, and cooling channels as shown in Figure 1 and injection speed is exhibited in Figure 2. Mold temperature at the interface between the inserted film and mold cavity was 32°C and mold temperature at the interface between injected resin and mold cavity was 43°C. Multiple packing process was used such that packing pressure of 60 MPa was applied for the first 9.8 seconds and 90 MPa for the next 0.2 seconds. After ejection, the molded part was annealed in a convection oven at 80°C for 5 days to estimate viscoelastic deformation of the part. Two abbreviations were used for the specimens in this study, i.e., FIM-E and FIM-A represent film insert molded specimen after ejection and after annealing, respectively. The warpage was measured before and after annealing by scanning the parts with a 3D scanner (3D NEXTUS, Chung-ju City, Chung Cheongbuk-Do, Korea).

Measurement of residual stresses

Various measurement methods have been developed for determination of residual stress. The layer-removal method, which was developed by Treutin and Read[13] is one of the most commonly reliable destructive methods but is limited to the measurement of residual stresses in flat plates. It is impossible to apply the technique to an object with complex geometry.[13–16] On the other hand, the hole-drilling method is applicable to an object with a complex geometry and have been used to evaluate residual stresses in complex automotive interior parts.[17] The hole-drilling method is a semi-destructive residual stress measurement technique which was first proposed by Mathar.[18] When a hole is drilled and the material is removed, a new stress equilibrium is established around the hole by the stress relaxation. Localized stress relaxation is caused by deformation around the hole as soon as the stressed material is removal. Generation of the strain caused by the deformation can be measured by using a specially designed strain gage, rosette. The procedure is relatively simple and has been standardized as depicted in the ASTM Standard Procedure E 837.

The experimental set-up used previously for the hole-drilling method was used.[19,20] A special three-element strain gage, rosette (062UL type, Measurement Group, Culver City, CA), was installed on the surface of the parts at the point where residual

Figure 3 Complex automotive interior part showing the location where the residual stress distribution was measured. [Color figure can be viewed in the online issue, which is available at www.interscience.wiley.com.]

stresses were to be determined. Figure 3 shows the complex automotive interior part and the location where the residual stress distribution was measured with respect to depth by using the hole drilling method. A precision milling guide (RS-200, Measurement Group) was attached to the part and centered accurately over a drilling target in the rosette. The induced strain can be measured at each drilling step and the relationship between the principal strain and stress is considered to determine the level of residual stresses.[21,22] In the present study, the integral method was used to measure the residual stresses because it was appropriate to evaluate the residual stress variation for each increment in thickness direction during the incremental hole-drilling.[23–25]

The elastic strain, ε_{rr}, was measured by the rosette at the periphery of the hole and is related to the principal stresses by the following equation:

$$\varepsilon_{rr} = \left(\bar{A} + \bar{B}\cos 2\beta\right)\sigma_{\max} + \left(\bar{A} - \bar{B}\cos 2\beta\right)\sigma_{\min}, \quad (2)$$

$$\bar{A} = -\frac{\bar{a}(1+\nu)}{2E}, \quad \bar{B} = -\frac{\bar{b}}{2E}, \quad (3)$$

where $\sigma_{\max}$ and $\sigma_{\min}$ are principal stresses, β is an angle measured counterclockwise from the maximum principal stress direction to the axis of the strain gage, $\bar{A}$ and $\bar{B}$ are calibration constants, $\bar{a}$ and $\bar{b}$ are dimensionless constants, E is Young's modulus, and v is Poisson's ratio. Magnitude and direction of the two principal stresses are obtained in terms of the measured strains.

$$\sigma_{\max}, \sigma_{\min} = \frac{\varepsilon_1 + \varepsilon_3}{4\bar{A}} \mp \frac{\sqrt{(2\varepsilon_2 - \varepsilon_1 - \varepsilon_3)^2 + (\varepsilon_1 - \varepsilon_3)^2}}{4\bar{B}} \quad (4)$$

$$\beta = \frac{1}{2}\tan^{-1}\left(\frac{2\varepsilon_2 - \varepsilon_1 - \varepsilon_3}{\varepsilon_1 - \varepsilon_3}\right) \quad (5)$$

where ε_1, ε_2, and ε_3 are relaxed strains measured by the strain gage.[26–28]

NUMERICAL SIMULATION

Three-dimensional numerical analysis was used to predict melt front advancement into the cavity and development of residual stresses of the part because the film insert molded part consists of film and substrate domains. Three-dimensional simulation of the injection molding was required especially for numerical analysis of the viscoelastic deformation of the film insert molded part. A mesh generating program, HyperMesh, was used to generate two dimensional finite element meshes for film and substrate domains of the part. The two dimensional finite elements were created separately for each domain and three dimensional finite elements were fully generated after they were transported to Moldflow and combined together.

TABLE I
Material Properties of the Film and Resin Used for Numerical Simulation

	Film (Techno ABS545)	Resin (Lupoy HR 5007AB)
Elastic modulus (MPa)	2240	2780
Poisson's ratio	0.392	0.23
Melt density (kg/m^3)	943.9	1003.6
Solid density (kg/m^3)	1054.1	1136.7
Thermal expansion coefficient (K^{-1})	8×10^{-5} (or -4.2×10^{-5})	6.7×10^{-5}
Thermal conductivity (W/m·K)	0.116 (at 75°C, temperature dependent)	0.21 (at 79°C, temperature dependent)
Specific heat (J/kg·K)	2202 (at 200°C, temperature dependent)	2205 (at 265°C, temperature dependent)

Flow analysis

The governing equations for the flow analysis in the mold cavity are the conservation of mass, conservation of momentum, and conservation of energy equations[29] as shown below.

$$\frac{D\rho}{Dt} + \rho(\nabla \cdot v) = 0 \quad (6)$$

$$\rho\frac{Dv}{Dt} = -\nabla P + \nabla \cdot \tau + \rho g \quad (7)$$

$$\rho C_p \frac{DT}{Dt} = \beta T \frac{DP}{Dt} + \eta\dot{\gamma}^2 + \nabla \cdot q \quad (8)$$

where ρ is density, v is velocity vector, P is pressure, τ is viscous stress tensor, g is gravity/body-force vector, C_p is specific heat at constant pressure, β is expansivity, ν is generalized Newtonian viscosity, q is heat flux, and $\dot{\gamma}$ is the shear rate,

$$\dot{\gamma} = \sqrt{\left(\frac{\partial u}{\partial z}\right)^2 + \left(\frac{\partial v}{\partial z}\right)^2} \quad (9)$$

where u and v are the velocity components in the x and y directions. The flow front in the cavity is tracked using a fluid concentration equation, which can be expressed as

$$\frac{DF}{Dt} = 0 \quad (10)$$

where F is fluid concentration. Because inserts are treated as a rigid body with no deformation or displacement, mass and momentum conservation in inserts are ignored. However, heat exchange

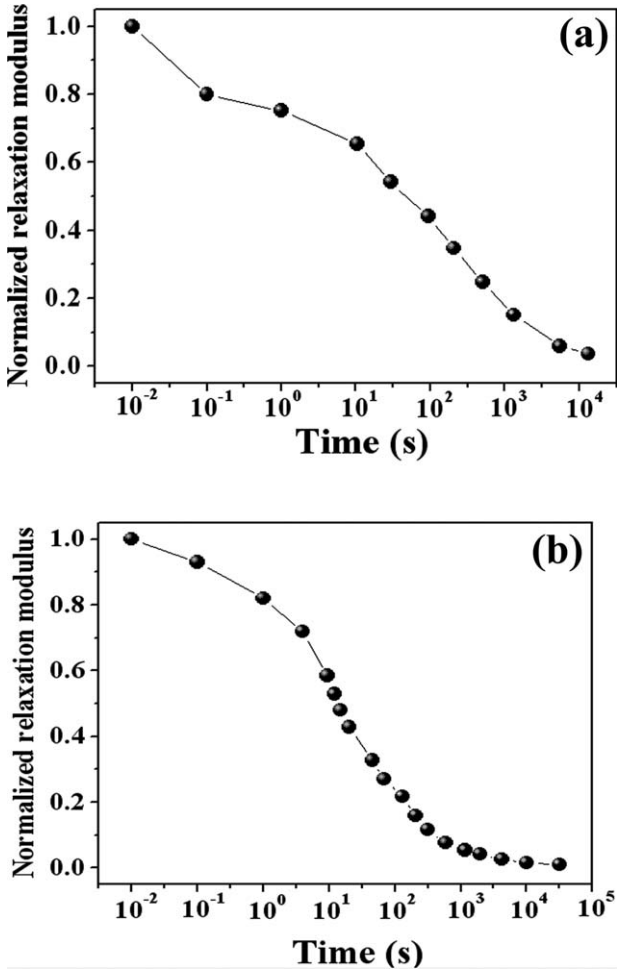

Figure 4 Normalized relaxation moduli of (a) the PMMA/ABS laminated film and (b) PC/ABS blend substrate.

between the inserted film and mold or polymer melt needs to be evaluated. Hence energy balance in the process must be taken into account. The only equation relevant to the insert is the conservation of energy. By using the assumption that the insert is a rigid body, the conservation of energy equation for the cavity given in eq. (8) can be simplified for inserts and is represented as,[29]

$$\rho C_p \frac{\partial T}{\partial t} = \nabla \cdot q \tag{11}$$

Three-dimensional flow analysis was performed by assuming that rheological behavior of the polymeric melt satisfies the modified Cross model with the following Williams-Landel-Ferry (WLF) equation.[29,30]

$$\eta = \frac{\eta_0}{1 + \left(\frac{\eta_0 \dot{\gamma}}{\tau^*}\right)^{(1-n)}} \tag{12}$$

$$\log \frac{\eta_0 \theta^* \rho^*}{\eta^* \theta \rho} = \frac{-C_1(\theta - \theta^*)}{C_2 + (\theta - \theta^*)}$$

where η is viscosity, η_0 is zero shear rate viscosity, $\dot{\gamma}$ is shear rate, τ^* is shear stress at the transition between Newtonian and power law behavior, η^* is viscosity at reference temperature, ρ is density, ρ^* is density at reference temperature, θ is temperature, and θ^* is reference temperature. Typically θ^* is chosen as the glass transition and $C_1 = 17.44$ and $C_2 = 51.6$ K for many polymers. Heat conduction through the mold polymer interface, convective heat transfer by the cooling liquid, and viscous heating during both filling and post-filling stages should be considered in the thermal analysis. The modified Tait equation is used as the PVT relationship. The thermal and flow fields are calculated with the control-volume approach to handle the melt-front advancement by utilizing a hybrid FEM/ FDM scheme. An implicit numerical scheme is used to solve the discretized energy equation.[31]

Residual stresses were calculated by using the hybrid model.[29]

$$\sigma_e^{//} = b_1 \sigma_P + b_2 \tau + b_3$$
$$\sigma_e^{\perp} = b_4 \sigma_P + b_5 \tau + b_6 \tag{13}$$

where $\sigma_e^{//}$ and $\sigma_e^{\perp}$ are the corrected principal stresses in the directions parallel and transverse to flow respectively, σ_P is the predicted residual stress, $b_i's$ (where $i = 1,...6$) are constants to be determined and τ is a measure of orientation in the material.[29] The laminated film was treated as a homogeneous film by neglecting the PMMA layer because the PMMA layer is relatively thin. Properties of ABS (techno ABS 545, techno polymer) were used as properties of the film and those of the polymer resin (Lupoy HR5007AB, LG Chemical) were selected as properties of the injected resin for flow analysis. Selected material properties of the polymer resin and film are summarized in Table I. Molding conditions for the numerical predictions are the same as

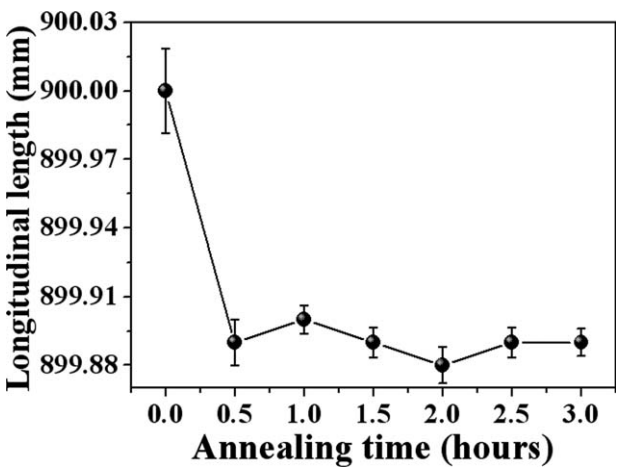

Figure 5 Dimensional variation of the film annealed at 80°C with respect to the annealing time.

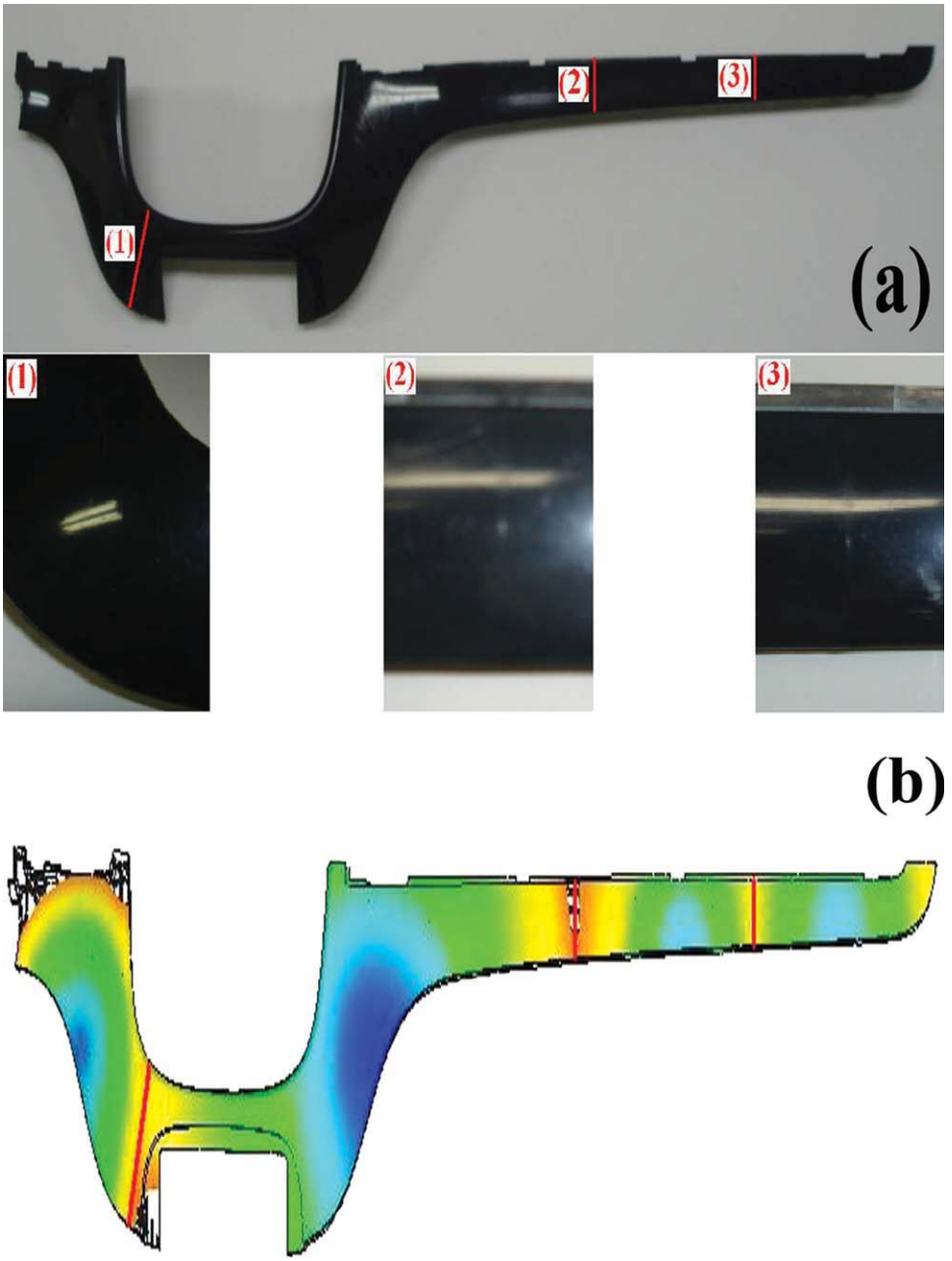

Figure 6 Comparison of (a) weld lines observed by the experiment and (b) predicted by the numerical simulation. [Color figure can be viewed in the online issue, which is available at www.interscience.wiley.com.]

the experimental conditions. At the end of the flow analysis, the output data was exported to the stress analysis program and the interface between the film and the substrate was joined. The in-mold stress condition of the part was exported to the stress simulation code and used as the initial condition for structural analysis of the film insert molded part.

Stress analysis

Residual stress distribution and deformation of the ejected FIM parts were predicted by applying elastic properties of the solid polymer. However, it is well known that viscoelastic properties must be applied to predict time-dependent deformation of polymeric parts, which are exposed to various environmental conditions. For prediction of long-term viscoelastic behavior of the polymeric part, it was assumed that the viscoelastic polymer material was isotropic and the temperature effect on material behavior was explained by the thermo-rheological simplification. Constitutive equation of the generalized Kelvin model was selected as the constitutive equation for the linear thermoviscoelastic material. The linear thermoviscoelastic constitutive equation is represented by hereditary integrals and the effect of

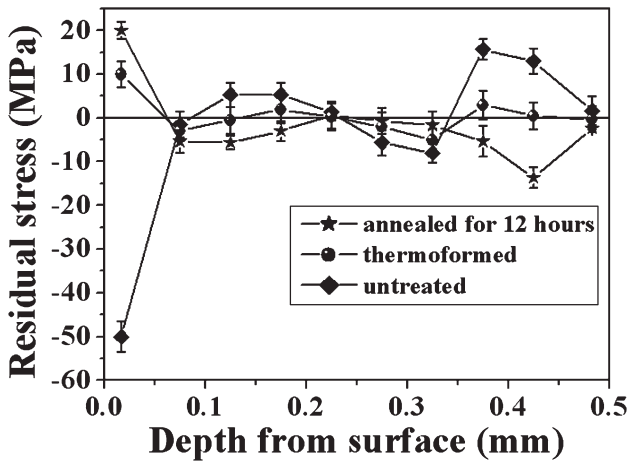

Figure 7 Residual stress distribution of the untreated film, thermoformed film, and annealed film treated at 80°C for 12 h.

temperature is considered by the following equation.[32,33]

$$\tau(t) = G_0(\theta)\left(\gamma - \int_0^t \dot{g}_R(\xi(s))\gamma(t-s)ds\right) \tag{14}$$

where the instantaneous shear modulus G_0 is temperature dependent and γ is the shear strain.

$$\dot{g}_R(\xi) = dg_R/d\xi$$
$$g_R(t) = G_R/G_0 \tag{15}$$

where $G_R(t)$ is the time dependent shear relaxation modulus that characterizes the material's response and $g_R(t)$ is dimensionless relaxation modulus. $\xi(t)$ is the reduced time defined by the following equation.

$$\xi(t) = \int_0^t \frac{ds}{A(\theta(s))} \tag{16}$$

where $A(\theta(t))$ is a shift function at time t. Temperature dependence of the reduced time is usually referred to as the thermo-rheologically simple (TRS) temperature dependence. The shift function is often approximated by the WLF form.

$$\log(A) = \log\left(\frac{t}{t_0}\right) = \frac{-C_1'(\theta-\theta^*)}{C_2' + (\theta-\theta^*)} \tag{17}$$

where θ^* is the reference temperature at which the relaxation data are provided and C_1' and C_2' are calibration constants obtained at the temperature.

$$C_1' = \frac{C_1^g}{1 + (\theta^* - \theta_g)/C_2^g}, \quad C_2' = C_2^g + \theta^* - \theta_g \tag{18}$$

where C_1^g and C_2^b are universal constants, which are 17.4 and 51.6 K, respectively. Normalized relaxation moduli of the substrate and the film were measured as shown in Figure 4 and used for the isotropic viscoelastic stress analysis. The relaxation moduli were measured by varying the temperature from 25 to 100°C and the master curve was constructed by applying the shift function.[34]

The ejection step was established by solving an elastic problem when fixed boundary conditions are eliminated suddenly and the annealing step was dealt with by assuming that the part was kept at 80°C for 5 days. Thermal expansion coefficient of the inserted film was determined by experiments as -1.826×10^{-6} K^{-1} for numerical modeling of the annealing until the first annealing step was over. The thermal expansion coefficient was negative because the film shrank due to irreversible relaxation of the molecular orientation, which had been developed by biaxial drawing during film manufacturing. Figure 5 shows the dimensional change of the film with respect to increasing annealing time when annealed at 80°C. The thermal expansion coefficient was obtained from the experimental data by using the eq. (1). After the first annealing step, thermal expansion coefficient of the film was reset by that of the annealed film (8×10^{-5} K^{-1}) because most of the molecular orientation in the film had been released during annealing.

RESULTS AND DISCUSSION

Precise flow analysis of the FIM process is important for accurate prediction of residual stresses and viscoelastic deformation of film insert molded parts. The flow analysis can predict weld line locations, which are usually observed experimentally. Because of complex geometry of the part, quadruple gate system was used and three weld lines were generated in the part. Figure 6 shows weld lines observed in

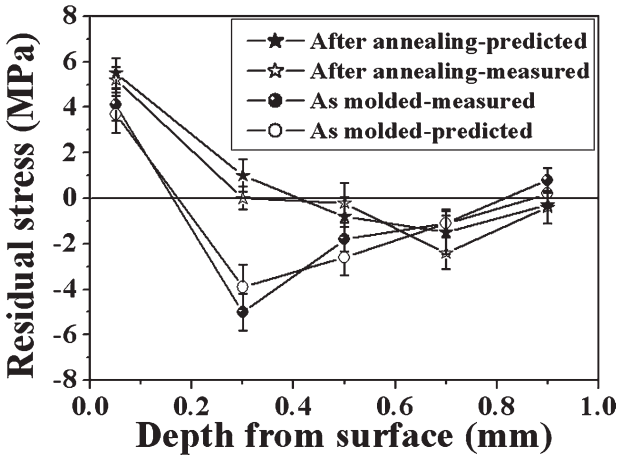

Figure 8 Residual stress distribution of the molded automotive part and the annealed part treated at 80°C for 20 days.

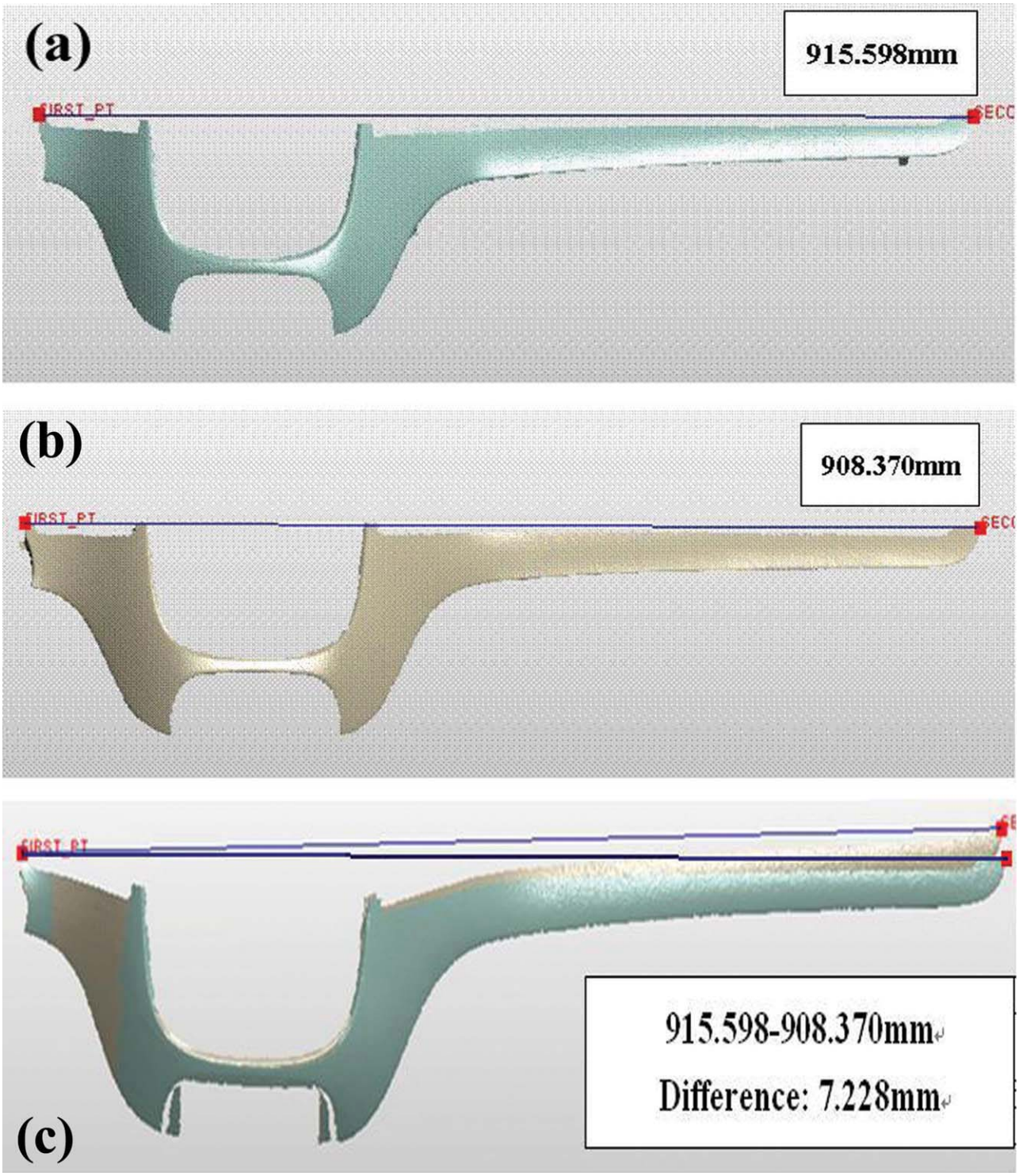

Figure 9 Deformed geometry of (a) the FIM-E part after ejection, (b) the FIM-A part annealed at 80°C for 5 days, and (c) longitudinal length difference between FIM-E and FIM-A specimens. [Color figure can be viewed in the online issue, which is available at www.interscience.wiley.com.]

the molded part and predicted by the flow simulation. The weld lines are located almost at the same positions when the predicted results are compared with the experimental results, which implies that the flow analysis was performed properly.

Residual stresses should be analyzed to predict and understand deformation of the molded parts. Residual stress distribution of the unannealed pristine film as well as the thermoformed film is shown with respect to the depth in Figure 7. Although the residual

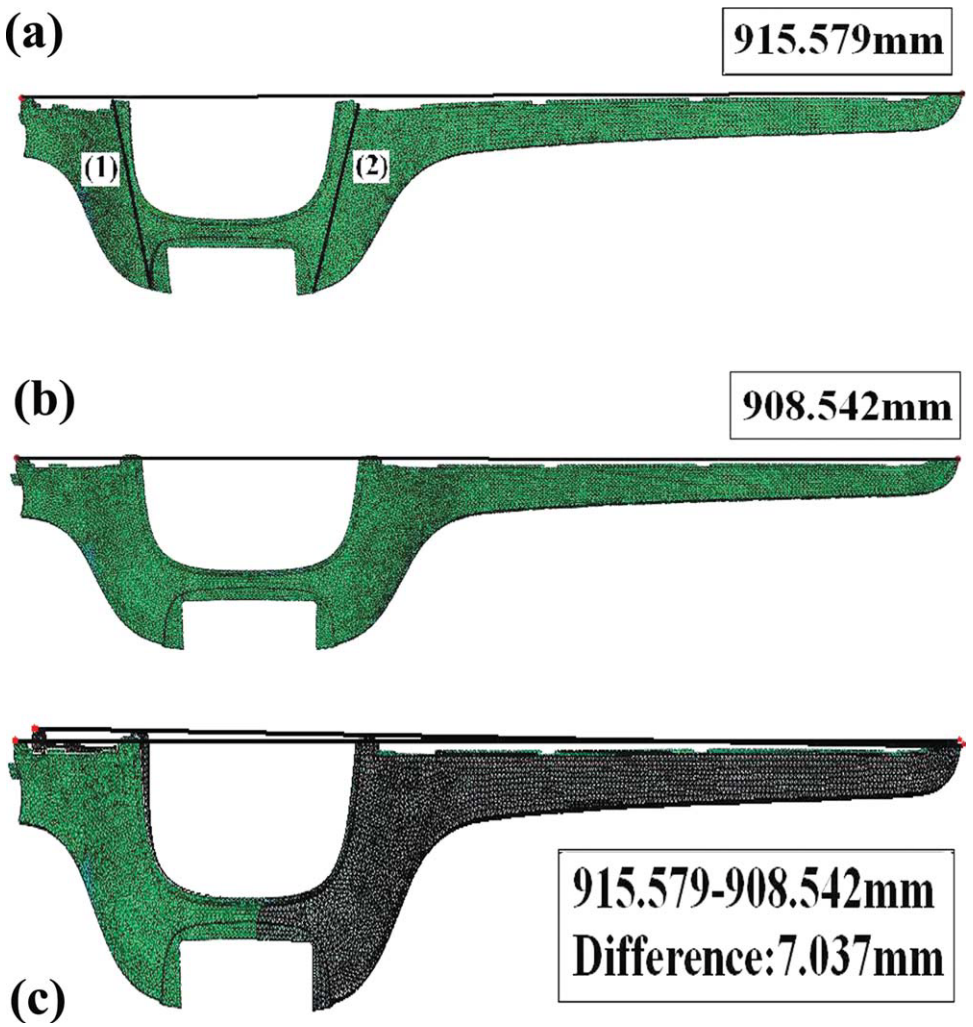

Figure 10 Numerically predicted geometry of (a) the FIM-E part after ejection, (b) the FIM-A part annealed at 80°C for 5 days, and (c) longitudinal length difference between FIM-E and FIM-A specimens. The lines (1) and (2) are explained in Table II. [Color figure can be viewed in the online issue, which is available at www.interscience.wiley.com.]

stress distribution of the unannealed pristine film was varied as compression, tension, compression, and tension from the PMMA layer to the ABS layer, that of the thermoformed film was varied as tension and compression. The result was attributed to the fact that the residual stresses in the unannealed film had been relaxed during thermoforming process and new residual stress distribution was developed in the film by the different thermal expansion between PMMA and ABS layers. As shown in Figure 5, thermal shrinkage of the film was observed in the early stage of annealing because of thermal relaxation of the molecular orientation generated by the biaxial drawing performed in the film manufacturing. The residual stress of the film annealed for 12 h was also varied from tension to compression with respect to the depth. Larger tensile stresses of the PMMA layer can be also explained by the relaxation of the PMMA layer during annealing process.

Figure 8 shows both measured and predicted residual stress distributions of the ejected parts and the annealed parts treated at 80°C for 20 days. Residual stress distribution of the unannealed part was varied as tension, compression, and tension from the PMMA layer to the upper PC/ABS layer and the residual stress distribution of the annealed part was varied as tension and compression from the surface. Large tensile stresses were observed at the surface of the annealed part due to the relaxation of remained biaxial molecular orientation in the PMMA layer of the thermoformed film. Residual stresses in the film and substrate had been relaxed during annealing and the measured residual stress distribution was in good agreement with the predicted results. Therefore, numerical analysis of the FIM can be used for prediction of the geometry and residual stresses of the molded part.

Deformed geometry of the ejected part can be predicted by considering residual stresses developed in

TABLE II
Length of the Lines (1) and (2) Shown in Figure 10 (a): Comparison Between Experimental and Numerical Results

	After ejection		After annealing	
Lines	Exp.	Num.	Exp.	Num.
(1)	177.66	177.15	174.04	174.24
(2)	167.77	167.32	164.81	165.01

the part and viscoelastic structural analysis can be carried out by applying the deformed geometry and time-temperature superposition principle. Deformed geometry of the molded part after ejection (FIM-E) and that of the part annealed at 80°C for 5 days (FIM-A) are shown in Figure 9(a,b), respectively. The FIM-E was deformed such that the surface at the film side was protruded because shrinkage of the solid film was lower than that of the other side where polymer melt had been solidified by the cold surface of the mold. However, shape of the FIM-A was bent in the opposite direction such that the film surface was intruded. In Figure 9(c), difference in the longitudinal length of the part between FIM-E and FIM-A samples is displayed in one figure to identify annealing effect and the difference was 7.228 mm. In the previous study,[9,10] warpage reversal phenomena (WRP) was observed, i.e., film insert molded tensile specimens with the unannealed film were bent such that the film side was protruded and the warpage was reversed gradually during annealing such that the film side was intruded. The WRP occurred by the combined effect of thermal shrinkage of the inserted film and relaxation of residual stresses in the specimen during annealing.

Deformed geometry of the FIM-E and FIM-A specimens was calculated numerically and shown in Figure 10(a,b), respectively. In Table II, predicted and experimental results on the length of the parts are compared after ejection and annealing of the specimens. Although the film insert molded part is large and has a complex shape, the numerically predicted shape showed almost the same geometry as the experimental one as shown in Figure 10. Proper thermal expansion coefficients should be determined for numerical analysis of FIM and the WRP, which is caused by the irreversible relaxation of the molecular orientation. Viscoelastic behavior of the film insert molded part can be predicted by using the shift function based on the time-temperature superposition principle. According to the previous studies,[9–12] numerical analysis on FIM of a simple tensile specimen was conducted and provided good predictions on residual stresses and viscoelastic deformation. Warpage of film insert molded parts with complex geometry can be predicted by using the three dimensional numerical analysis used in this study.

CONCLUSIONS

Complex automotive interior parts were prepared by the FIM to investigate development of residual stresses and effects of viscoelastic deformation on warpage of the part. Three dimensional flow and stress analyses were performed for the large and complex automotive interior part to predict residual stresses, viscoelastic deformation, and warpage. Experimental results showed that thermal shrinkage of the inserted film and relaxation of the residual stresses imposed significant effect on the viscoelastic deformation of the part during annealing. Although the film insert molded part is large and has complex geometry, residual stresses, viscoelastic deformation, and warpage of the part were predicted and the numerical results showed good agreement with experimental results.

References

1. Leong, Y. W.; Kotaki, M.; Hamada, H. J Appl Polym Sci 2007, 104, 2100.
2. Leong, Y. W.; Ishiaku, U. S.; Kotaki, M.; Hamada, H. Polym Eng Sci 2006, 46, 1674.
3. Yamaguchi, S.; Leong, Y. W.; Tsujii, T.; Mizoguchi, M.; Ishiaku, U. S.; Hamada, H. J Appl Polym Sci 2005, 98, 294.
4. Leong, Y. W.; Yamaguchi, S.; Mizoguchi, M.; Hamada, H.; Ishiaku, U. S.; Tsujii, T. Polym Eng Sci 2004, 44, 2327.
5. Fischer, J. M. Handbook of Molded Part Shrinkage and Warpage; William Andrew Inc.: Norwich, 2003.
6. Kramschuster, A.; Cavitt, R.; Ermer, D.; Chen, Z.; Turng, L.-S. Polym Eng Sci 2005, 45, 1408.
7. Liao, S. J.; Hsieh, W. H. Polym Eng Sci 2004, 44, 2029.
8. Fan, B.; Kazmer, D. O.; Bushko, C.; Theriault, R. P.; Poslinski, A. J. J Polym Sci Part B: Polym Phys 2003, 41, 859.
9. Kim, S. Y.; Kim, S. H.; Oh, H. J.; Lee, S. H.; Baek, S. J.; Youn, J. R.; Lee, S. H.; Kim, S.-W. J Appl Polym Sci 2009, 111, 642.
10. Kim, S. Y.; Lee, S. H.; Baek, S. J.; Youn, J. R. Macromol Mater Eng 2008, 293, 969.
11. Baek, S. J.; Kim, S. Y.; Lee, S. H.; Youn, J. R.; Lee, S. H. Fiber Polym 2008, 9, 747.
12. Kim, S. Y.; Oh, H. J.; Kim, S. H.; Kim, C. H.; Lee, S. H.; Youn, J. R. Polym Eng Sci 2008, 48, 1840.
13. Treutin, R. G.; Read, W. T. Jr., J Appl Phys 1951, 22, 130.
14. Kim, S. K.; Lee, S. W.; Youn, J. R. Korea-Australia Rheol J 2002, 14, 107.
15. Zoetelief, W. F.; Douven, L. F. A.; Ingen Housz, A. J. Polym Eng Sci 1996, 36, 1886.
16. Hastenberg, C. H. V.; Wildervanck, P. C.; Leenen, A. J. H. Polym Eng Sci 1992, 32, 506.
17. Kim, S. Y.; Kim, C. H.; Kim, S. H.; Oh, H. J.; Youn, J. R. Polym test 2009, 28, 500.
18. Mathar, J. Trans ASME 1934, 56, 249.
19. Kim, C. H.; Youn, J. R. Polym test 2007, 26, 862.
20. Kim, C. H.; Kim, S.; Oh, H.; Youn, J. R. Fiber Polym 2007, 8, 443.
21. ASTM International. Determining Residual Stresses by the Hole-Drilling Strain-Gage Method, Annual Book of ASTM E837-01. ASTM International: West Conshohocken, 2001.

22. Measurement Group. Measurement of Residual Stresses by the Hole-Drilling Strain Gage Method, Tech Note TN-503-5. Measurement Group: North Carolina, 1993.
23. Wang, T.; Young, W. Eur Polym J 2005, 41, 2511.
24. Maxwell, A. S.; Turnbull, A. Polym test 2003, 22, 231.
25. Sicot, O.; Gong, X. L.; Cherouat, A.; Lu, L. J Compos Mater 2003, 37, 831.
26. Schajer, G. S. J Eng Mater-T ASME 1988, 110, 338.
27. Flaman, M. T.; Manning, B. H. Exp Mech 1985, 25, 205.
28. Schajer, G. S. J Eng Mater-T ASME 1981, 103, 157.
29. Kennedy, P. Flow Analysis Reference Manual; Moldflow Pty. Ltd.: Australia, 1993.
30. Macosko, C. W. Rheology, Principles, Measurements, and Applications; Wiley-VCH Inc.: New York, 1994.
31. Santhanam, N.; Chiang, H. H.; Himasekhar, K.; Tuschak, P.; Wang, K. K. Adv Polym Tech 1991, 11, 77.
32. Flűgge, W. Viscoelasticity; Springer-Verlag: New York, 1975.
33. Analysis User's Manual. ABAQUS Inc.; Rhode Island, 2003; Vol. 3.
34. Hong, S. J.; Yu, W.-R.; Youk, J. H.; Cho, Y. R. Fiber Polym 2007, 8, 377.